Science of the Total Environment 622–623 (2018) 88–95

Contents lists available at ScienceDirect

Science of the Total Environment

journal homepage: www.elsevier.com/locate/scitotenv

Fe^{3+}-saturated montmorillonite effectively deactivates bacteria in wastewater☆

Chao Qin, Chaoqi Chen, Chao Shang, Kang Xia *

Department of Crop and Soil Environmental Sciences, Virginia Polytechnic Institute and State University, Blacksburg, VA 24061, United States

HIGHLIGHTS

- Fe^{3+}-saturated montmorillonite's antibacterial activity was studied.
- Wastewater bacteria was deactivated effectively by Fe^{3+}-saturated montmorillonite.
- Fe^{3+}-saturated montmorillonite deactivated bacteria possibly by cell membrane damage.
- Fe^{3+}-saturated montmorillonite can disinfect bacteria-contaminated water.

GRAPHICAL ABSTRACT

The graphic abstract figure is only for simple demonstration of possible reaction processes. Sizes of different components do not reflect their actual relative scales.

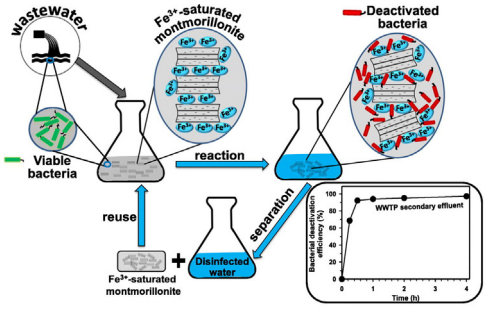

Notes: The graphic abstract figure is only for simple demonstration of possible reaction processes. Sizes of different components do not reflect their actual relative scales.

ARTICLE INFO

Article history:
Received 5 July 2017
Received in revised form 15 November 2017
Accepted 27 November 2017
Available online xxxx

Editor: H.M. Solo-Gabriele

Keywords:
Bacterial deactivation
Antibacterial activity
Montmorillonite
Wastewater treatment
Disinfection

ABSTRACT

Existing water disinfection practices often produce harmful disinfection byproducts. The antibacterial activity of Fe^{3+}-saturated montmorillonite was investigated mechanistically using municipal wastewater effluents. Bacterial deactivation efficiency (bacteria viability loss) was 92 ± 0.64% when a secondary wastewater effluent was mixed with Fe^{3+}-saturated montmorillonite for 30 min, and further enhanced to 97 ± 0.61% after 4 h. This deactivation efficiency was similar to that when the same effluent was UV-disinfected before it exited a wastewater treatment plant. Comparing to the secondary wastewater effluent, the bacteria deactivation efficiency was lower when the primary wastewater effluent was exposed to the same dose of Fe^{3+}-saturated montmorillonite, reaching 29 ± 18% at 30 min and 76 ± 1.7% at 4 h. Higher than 90% bacterial deactivation efficiency was achieved when the ratio between wastewater bacteria population and weight of Fe^{3+}-saturated montmorillonite was at $<2 \times 10^3$ CFU/mg. Furthermore, 99.6–99.9% of total coliforms, *E. coli*, and enterococci in a secondary wastewater effluent was deactivated when the water was exposed to Fe^{3+}-saturated montmorillonite for 1 h. Bacterial colony count results coupled with the live/dead fluorescent staining assay observation suggested that Fe^{3+}-saturated montmorillonite deactivated bacteria in wastewater through two possible stages: electrostatic sorption of bacterial cells to the surfaces of Fe^{3+}-saturated montmorillonite, followed by bacterial deactivation due to mineral surface-catalyzed bacterial cell membrane disruption by the surface sorbed Fe^{3+}. Freeze-drying the recycled Fe^{3+}-saturated montmorillonite after each usage resulted in 82 ± 0.51% bacterial deactivation efficiency

☆ The first two coauthors contributed to the manuscript equally and shall be considered as co-first authors.

* Corresponding author at: 1880 Pratt Dr., Virginia Tech, Blacksburg, VA 24061, United States.
E-mail address: kxia@vt.edu (K. Xia).

http://dx.doi.org/10.1016/j.scitotenv.2017.11.302
0048-9697/© 2017 Elsevier B.V. All rights reserved.

even after its fourth consecutive use. This study demonstrated the promising potential of Fe^{3+}-saturated montmorillonite to be used in applications from small scale point-of-use drinking water treatment devices to large scale drinking and wastewater treatment facilities.

© 2017 Elsevier B.V. All rights reserved.

1. Introduction

Ensuring adequate access to clean water worldwide is one of the greatest global challenges in this century because 1.2 billion people throughout the world lack safe drinking water and millions of people die annually from diseases caused by harmful microorganisms in untreated or improperly treated drinking water (Shannon et al., 2008). Water disinfection practices such as chlorination, ozonation, and UV treatment are commonly used. However, chlorination and ozonation, used separately or combined, often result in disinfection by-products (Huang et al., 2005; Muller et al., 2012; Richardson and Postigo, 2011; Zha et al., 2014). Many of the disinfection by-products can pose negative impact to human health (Krasner et al., 2009).

In the past decade, various natural or engineered nanomaterials have been developed as antibacterial agents for water disinfection purpose. Those nanomaterials include silver nanoparticles (Dankovich and Gray, 2011; Morones et al., 2005; Panáček et al., 2006), copper and copper oxide nanoparticles (Ben-Sasson et al., 2013; Meghana et al., 2015), titanium dioxide (Li et al., 2012; Simon-Deckers et al., 2009), carbon nanotubes (Tiraferri et al., 2011; Vecitis et al., 2010), zinc oxide (Applerot et al., 2009; Raghupathi et al., 2011), fullerenes (Lyon and Alvarez, 2008) and graphene materials (Hu et al., 2010; Liu et al., 2012; Perreault et al., 2015; Wu et al., 2013). Among them, silver-based nanomaterials have been most widely explored owing to their antibacterial properties to a broad spectrum of microorganisms (Panáček et al., 2006). The antibacterial activity of silver-based nanomaterials is mainly attributed to the release of Ag^{+}, which further interacts with the thiol functional groups in proteins, resulting in respiratory enzymes inactivation and reactive oxygen species generation (Matsumura et al., 2003). Furthermore, Ag^{+} can also prevent DNA replication and enhance detachment of cytoplasm membrane from cell wall (Feng et al., 2000). Silver-based antibacterial materials, however, can be expensive and have poor stability (Lv et al., 2010). There have been concerns about their long term efficacy and economic applicability (Qu et al., 2012). Previous research has shown that clay minerals have high specific surface area, cation exchange capacity, and sorption capacity and, therefore, result in their high sorption capacity for cations including Ag^{+}, Zn^{2+}, and Cu^{2+}. Research has shown that clay minerals modified with these cations possess antibacterial property (Hrenovic et al., 2012; Hu et al., 2005; Magana et al., 2008; Malachová et al., 2011; Morrison et al., 2014; Tong et al., 2005; Williams and Haydel, 2010). However, the effectiveness of Fe^{3+}-modified clay minerals for bacterial disinfection of contaminated water has not been tested.

Our previous studies have demonstrated effective removal of phenolic organic compounds from wastewater due to surface catalyzed oxidative oligomerization by Fe^{3+}-saturated montmorillonite (Liyanapatirana et al., 2009; Qin et al., 2014). It was therefore hypothesized for the current study that the surface reactivity of Fe^{3+}-saturated montmorillonite might also capable of deactivating bacteria in wastewater. Although Cu^{2+}, Zn^{2+} and Ag^{+} exchanged montmorillonite have shown antibacterial activity, the possible leaching of these cations into water could pose potential threat to public health due to their toxicity at high concentrations. In this study, we therefore proposed to develop Fe^{3+}-saturated montmorillonite as an alternative to disinfect water because iron is an essential element for human. The objectives of this study were: 1) to investigate the influence of exposure time and mineral concentration on the bacterial deactivation efficiency of Fe^{3+}-saturated montmorillonite; 2) to elucidate bacterial deactivation mechanisms when exposed to Fe^{3+}-saturated montmorillonite; and 3) to evaluate the performance stability and reusability of Fe^{3+}-saturated montmorillonite for bacterial deactivation. To achieve these objectives, a wide spectrum of culturable bacteria associated with the primary and secondary effluents from a local wastewater treatment plant and water quality indicator bacteria including total coliforms (gram-negative), *E. coli* (gram-negative) and enterococci (gram-positive) were tested. Because the main focus of this study was to investigate if Fe^{3+}-saturated montmorillonite is capable of deactivating wastewater bacteria, differentiation of spore-forming bacteria vs. non-spore-forming bacteria is beyond the scope of this study.

2. Materials and methods

2.1. Chemicals and materials

Luria-Bertani (LB) broth powder (Lennox), agar powder, sodium chloride (≥99%) were purchased from Fisher Scientific (Fair Lawn, NJ). Na^{+}-montmorillonite (SWy-2, Crook County, Wyoming) was obtained from the Source Clays Repository of the Clay Minerals Society (Purdue University, West Lafayette, IN). The ultrapure water used in this study was produced by a Millipore Milli-Q water purification system (Milford, MA).

2.2. Fe^{3+}-saturated montmorillonite preparation

Detailed description for preparation of Fe^{3+}-saturated montmorillonite can be found in previous studies (Liyanapatirana et al., 2009; Qin et al., 2014). Briefly, Na^{+}-montmorillonite (Na^{+} as major interlayer cation) was first purified and fractionated to <2 μm clay-sized particles and then went through six saturation-decantation cycles using 0.1 M $FeCl_3$ to saturate the montmorillonite interlayers with Fe^{3+}. The Fe^{3+}-saturated montmorillonite was then repeatedly washed with ultrapure grade water followed by centrifugation until no Cl^{-} in the supernatant was detected using the $AgNO_3$ test. The washed Fe^{3+}-saturated montmorillonite was finally freeze-dried for future tests of its antibacterial efficiency.

2.3. Bacterial deactivation study using Fe^{3+}-saturated montmorillonite

To prevent bacterial cross contamination during each step of testing, all related glassware and materials were properly sterilized by autoclaving at 121 °C for 20 min. Two milliliters of primary or secondary wastewater effluent from a local wastewater treatment plant was mixed with a predetermined amount (varied from 5 mg to 70 mg depending on the experiment) of Fe^{3+}-saturated montmorillonite in a 20 mL glass vial and shaken on a horizontally moving shaker at 200 rpm for up to 4 h at 25 °C. To compare results, the amount of Fe^{3+}-saturated montmorillonite was normalized to the volume of wastewater treated, resulting in mineral concentrations of 2.5–35 mg/mL. Specific concentrations are stated in the figures and results. This conventional wastewater treatment plant treats domestic wastewater by sequentially using primary sedimentation, secondary biological activated sludge treatment, and UV disinfection (medium pressure high intensity mercury arc lamp) before the treated water is discharged into a receiving river. The effluent from the primary sedimentation tank, the secondary biological treatment basin before UV disinfection, and the UV disinfection basin were used for the experiment without any modification. The characteristics of the primary and secondary wastewater effluents are summarized in Table 1. At 0.5 h, 1 h, 2 h and 4 h, triplicate vials were taken from the

shaker and centrifuged at 1000 rpm for 5 min to separate the aqueous phase and mineral phase. Supernatant (aqueous phase) of each vial was withdrawn and weighed. The amount of water trapped in the mineral sediment was calculated by the difference between the weight of the mineral and what was initially added into each vial. This was included in the later calculation of aqueous phase bacterial population and excluded in the calculation of mineral phase bacterial population.

Bacterial populations, expressed in colony forming unit (CFU), in the wastewater samples, the aqueous phase, and the mineral phase were quantified using the Colony Forming Count method (Pepper and Gerba, 2015). Briefly, a wastewater or an aqueous phase sample was diluted sequentially 10-fold with saline water (0.85% NaCl) for up to 5 times. An aliquot of 100 μL was taken from each diluted solution, spread onto a pre-sterilized LB agar growth media, and incubated at 28 °C for 24 h before colony counting. The LB agar growth media is commonly used for lab culturing of a wide range of bacteria including pathogenic bacteria such as *E. coli* and *Staphylococcus aureus* (Hrenovic et al., 2012; Tang et al., 2013). The collected mineral phase was re-suspended in 10 mL sterilized saline solution, hand mixed thoroughly for 1 min, sequentially diluted 10-fold using saline water (0.85% NaCl) for up to 5 times, followed by the colony forming count for each diluted mixture using the plate cultural method as described above. The sum of the bacterial populations in the aqueous phase and the mineral phase was calculated as total CFU and compared with that in the wastewater before it was exposed to Fe^{3+}-saturated montmorillonite or Na^{+}-montmorillonite. The bacterial deactivation efficiency was calculated as $((C_o - C_t)/C_o) \times 100\%$, where C_t is the total CFU at different reaction time t, C_o is the CFU of the wastewater used. To test the reusability of Fe^{3+}-saturated montmorillonite for bacterial deactivation in wastewater, the Fe^{3+}-saturated montmorillonite sediment was collected after each deactivation cycle via centrifugation and used as is for the next cycle or freeze dried before being used for the next cycle, each with a fresh batch of wastewater sample. Four consecutive cycles were tested.

In addition to testing a wide range of wastewater associated culturable bacteria, deactivation efficiency of specific water quality indicator organisms including total coliforms, *E. coli*, and enterococci in the wastewater samples were also evaluated and tested using Quanti-Tray/2000 (IDEXX Laboratories, Westbrook, ME) following the USEPA approved Colilert and Enterolert tests for wastewater samples (APHA, 2012). Briefly, after 1 h exposure to Fe^{3+}-saturated montmorillonite (10 mg/mL), secondary wastewater sample was then mixed with one pack of colilert in sterile vessel, transferred to Quanti-Tray/2000, sealed using IDEXX Quanti-Tray sealer and finally incubated at 35 °C for 24 h. Quanti-Tray wells shown in yellow were counted and quantified as total coliforms using the IDEXX MPN Generator software. Quanti-Tray wells that were yellow and blue fluorescent under UV light (6 W, 365 nm) were counted as *E. coli*. Similarly, enterolert reagent pack was added into wastewater sample using same Quanti-Tray enumeration procedure. After incubation at 41 °C for 24 h, Quanti-tray wells that displayed blue fluorescence under UV light (6 W, 365 nm) were counted as enterococci positive.

2.4. Bacterial cell viability assay

Bacterial cell viability during the deactivation tests was further visualized using the fluorescence-based cell live/dead test (Perreault et al., 2015). An aliquot of 1 mL wastewater sample was incubated overnight in 25 mL LB growth medium at 28 °C until reaching mid-exponential growth phase. Bacteria in the growth medium were then harvested by centrifugation at 7500 rpm for 10 min. The bacterial pellet was washed twice using saline solution to remove residual macromolecules and other growth medium constituents. The bacterial pellet was first re-suspended in 2 mL wastewater, then exposed to 50 mg Fe^{3+}-saturated montmorillonite for 4 h, and finally centrifuged at 1000 rpm for 5 min. The mineral phase collected was re-suspended in 1 mL saline solution and stained by using the LIVE/DEAD BacLight bacterial viability kit (L7007, Invitrogen, Carlsbad, CA, USA). An aliquot of 3 μL dye mixture containing SYTO 9® and propidium iodide was added to the 1 mL mineral-saline mixture suspension and incubated in darkness for 15 min before final observation under a Zeiss fluorescence microscope (Axio Observer Z1, Carl Zeiss, Germany). With mixture of the SYTO 9® and propidium iodide (PI), bacteria with intact cell membranes stain fluorescent green (considered to be viable), and bacteria with compromised membranes stain fluorescent red (considered to be nonviable). Similar fluorescence dye methods have been applied in other studies monitoring the antibacterial properties of nanoparticles (Liu et al., 2009; Perreault et al., 2015; Raghupathi et al., 2011).

Table 1
Characteristics of the primary and secondary wastewater effluents used for this study.

Parameter	Primary	Secondary
pH	7.5	7.4
Dissolved oxygen (DO) (mg/L)	2.0	8.3
Biological oxygen demand (BOD) (mg/L)	77	2.9
Alkalinity (mg/L, $CaCO_3$)	227	113
Total suspended solids (mg/L)	53	2.5

2.5. Statistical analysis

Student's *t*-test was performed to determine whether there are significant differences in bacterial cell viability between different treatments. Statistical decisions were made at a significance level of $p < 0.05$ within a 95% confidence interval.

3. Results and discussion

3.1. Bacterial deactivation efficiency of Fe^{3+}-saturated montmorillonite

Without exposure to any treatment, bacterial populations in both primary and secondary wastewater effluents did not change significantly ($(((C_o - C_t) / C_o) \times 100\% = -12.4 \pm 22.1\%$ to $8.0 \pm 7.7\%$) during the 4-h testing time. When exposed to Na^{+}-montmorillonite at 35 mg/mL for up to 1 h, there was no statistically significant change in the bacterial populations in both primary and secondary wastewater effluents (Fig. 1). Incubation with Na^{+}-montmorillonite for longer than 1 h resulted in significant bacterial growth (negative values of bacterial deactivation efficiency), with $42 \pm 26\%$ and $117 \pm 38\%$ bacterial population enhancement in the primary and secondary wastewater effluents, respectively, at the end of 4-h incubation (Fig. 1). Growth stimulation of a wide spectrum of bacterial species by natural montmorillonite had been reported in the literature (Stotzky, 1966; Stotzky and Rem, 1966; Van Loosdrecht et al., 1990). It was speculated that the relative basicity of cations such as Na^{+} and Ca^{2+} sorbed on the Na^{+}-montmorillonite interlayer surfaces might provide the pH (5.5–7.0) environment and mineral nutrients, both are essential for bacterial metabolism and growth (Stotzky and Rem, 1966).

As shown in Fig. 1, bacteria in the secondary wastewater effluent were rapidly deactivated within 30 min of exposure to Fe^{3+}-saturated montmorillonite at 35 mg/mL, achieving deactivation efficiency of $69 \pm 3.2\%$ and $92 \pm 0.64\%$ after 15 and 30 min, respectively. Longer exposure of the secondary wastewater effluent to Fe^{3+}-saturated montmorillonite from 30 min to 4 h only slightly further enhanced the bacterial deactivation efficiency to $97 \pm 0.61\%$. Comparing to the secondary wastewater effluent, the bacterial deactivation efficiency was lower when the primary wastewater effluent was exposed to Fe^{3+}-saturated montmorillonite (35 mg/mL), reaching $29 \pm 18\%$ at 30 min and $76 \pm 1.7\%$ at 4 h.

The initial bacterial population in the primary wastewater effluent ($(1.39 \pm 0.0862) \times 10^5$ CFU/mL) was 6 times higher than that in the secondary wastewater effluent ($(2.33 \pm 0.201) \times 10^4$ CFU/mL). If bacterial deactivation is mineral surface dependent, higher ratio of bacterial

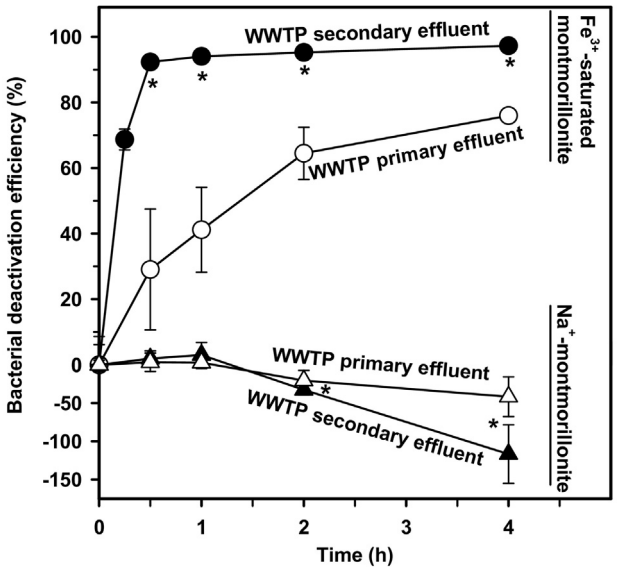

Fig. 1. Bacterial deactivation efficiencies of Fe^{3+}-saturated montmorillonite (circles) and Na^{+}-montmorillonite (upper triangles) when they were exposed to primary and secondary wastewater effluents for different length of time. The mineral concentration in the water was 35 mg/mL. The initial bacterial levels in the primary and secondary effluents were $(1.39 \pm 0.0862) \times 10^5$ and $(2.33 \pm 0.201) \times 10^4$ CFU/mL, respectively. * indicates statistical significant difference between the open and closed circles or upper triangles at a significance level of $p < 0.05$ within a 95% confidence interval.

population relative to the amount of Fe^{3+}-saturated montmorillonite they are exposed to would result in lower bacterial deactivation efficiency. Fig. 2a shows a significantly decreased bacterial deactivation efficiency, from 93 ± 0.71% to 16 ± 13%, when the ratio of wastewater bacterial population to Fe^{3+}-saturated montmorillonite increased from 2×10^3 to 9×10^3 CFU/mg. When this ratio decreased from 2×10^3 to 0.7×10^3 CFU/mg, the bacterial deactivation efficiency increased slightly from 93 ± 0.71% to 98 ± 0.83%. The results from Fig. 2a suggests that in order to achieve >90% bacterial deactivation efficiency, the bacterial population to Fe^{3+}-saturated montmorillonite ratio has to be below 2×10^3 CFU/mg. As a result, all subsequent experiments for secondary wastewater were conducted at Fe^{3+}-saturated montmorillonite concentration of 25 mg/mL. The ratio of primary wastewater bacterial population to Fe^{3+}-saturated montmorillonite

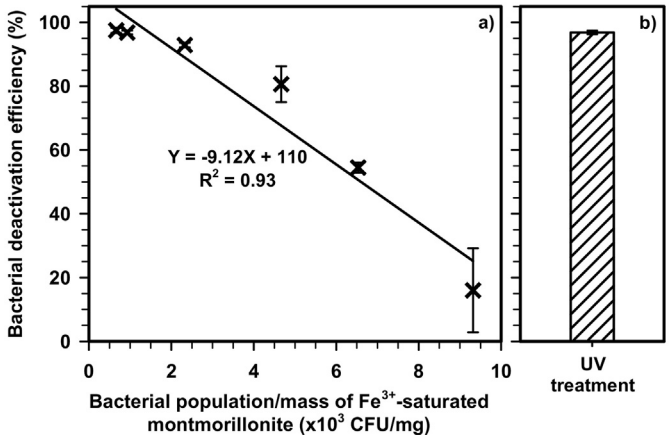

Fig. 2. (a) Bacterial deactivation efficiencies when an UV-untreated secondary wastewater effluent was exposed to Fe^{3+}-saturated montmorillonite for 2 h at different concentrations. The initial bacterial populations in the tested secondary effluent were consistently at $(3.27 \pm 0.779) \times 10^4$ CFU/mL, while the doses of the Fe^{3+}-saturated montmorillonite they were exposed to varied from 2.5–35 mg/mL. (b) The bacterial deactivation efficiency of UV treatment of the secondary wastewater effluent at the WWTP where the tested wastewater samples were collected.

was 4×10^3 CFU/mg, which would result in ~72% bacterial deactivation efficiency as predicted by the regression line shown in Fig. 2. This prediction matches well with the experimentally observed 2-h and 4-h bacterial deactivation efficiencies for the primary effluent (Fig. 1). To achieve >90% bacterial deactivation efficiency in the primary wastewater effluent tested for this study, the Fe^{3+}-saturated montmorillonite concentration would have to be at least 63 mg/mL. In contrast to the secondary wastewater effluent (Table 1), the primary wastewater effluent contains higher organic matter which may interfere with microorganism-mineral surface interactions (Huang, 2004; Katsoyiannis and Samara, 2007). The result from this study (Fig. 1) suggests that the Fe^{3+}-saturated montmorillonite is more suited for treating secondary wastewater effluent than primary wastewater effluent. Therefore, secondary wastewater became the focus of further investigation of this study. Fig. 2b shows that the bacterial deactivation efficiency of the UV treatment employed by the treatment plant to disinfect the secondary wastewater effluent was 99.9%. This outcome is comparable to that achieved by treating the secondary effluent with appropriate amount of Fe^{3+}-saturated montmorillonite treatment (Fig. 1 and Fig. 2a).

Fe^{3+}-saturated montmorillonite was further tested to deactivate common water quality indicator bacteria in wastewater. The initial concentrations of total coliforms, *E. coli* and Enterococci in secondary wastewater sample, tested using the Colilert and Enterolert method, were 3.4×10^5 MPN/100 mL, 1.6×10^4 MPN/100 mL and 3.8×10^3 MPN/100 mL, respectively. When exposed to Fe^{3+}-saturated montmorillonite at 10 mg/mL for 1 h, the deactivation efficiencies for total coliforms, *E. coli*, and enterococci in secondary wastewater effluent reached >99.9%, 99.9%, and 99.6%, respectively. Total coliforms and *E. coli* are gram-negative bacteria while enterococci is gram-positive bacteria. Although their cell wall structures are considerably different, similar deactivation efficiencies at >99.6% were achieved when the tested secondary wastewater effluent was exposed to Fe^{3+}-saturated montmorillonite. This result indicates that Fe^{3+}-saturated montmorillonite can deactivate a wide range of bacteria, as shown by the results on the culturable wastewater bacteria (Fig. 1).

The excellent bacterial deactivation efficiency of Fe^{3+}-saturated montmorillonite reported in our study is similar to that of other reported nanomaterials. It was reported that single-walled carbon nanotubes (50 mg/L) and graphene oxide (80 mg/L) could deactivate *E. coli* (~10^6 to 10^7 CFU/mL) after 4 h in aqueous environment at average efficiency of 88% and 92%, respectively (Kang et al., 2007; Liu et al., 2011). After immersion of silver nanoparticles-coated silicon wafers into *E. coli* and *S. aureus* inoculated growth medium for 12 h, 99% and 98% of *E. coli* and *S. aureus* (~2×10^5 CFU/mL) were deactivated, respectively (Zhou et al., 2014).

3.2. Distribution of viable bacteria between aqueous and mineral phases

Fig. 3 shows distribution patterns of viable wastewater bacteria in the primary and secondary effluents exposed to Fe^{3+}-saturated montmorillonite in comparison with Na^{+}-montmorillonite. Within 30 min exposure of the primary wastewater effluent to Fe^{3+}-saturated montmorillonite at 35 mg/mL, 4.8 ± 2.0% and 66 ± 14% of the initial wastewater bacterial population was detected as viable in the aqueous phase and mineral phase, respectively (Fig. 3a). From 30 min to 4 h exposure, the viable bacterial population associated with the Fe^{3+}-saturated montmorillonite mineral phase decreased significantly with time, while the viable bacterial population in the aqueous phase remains statistically unchanged. After 4 h exposure, only 21 ± 0.80% of the initial bacterial population was viable in the mineral phase. The result shown in Fig. 3a suggests that in the case of primary wastewater effluent, when the ratio of initial bacterial population to Fe^{3+}-saturated montmorillonite was high (Fig. 2a) and there might be high possibility of surface reaction interferences due to high organic matter content,

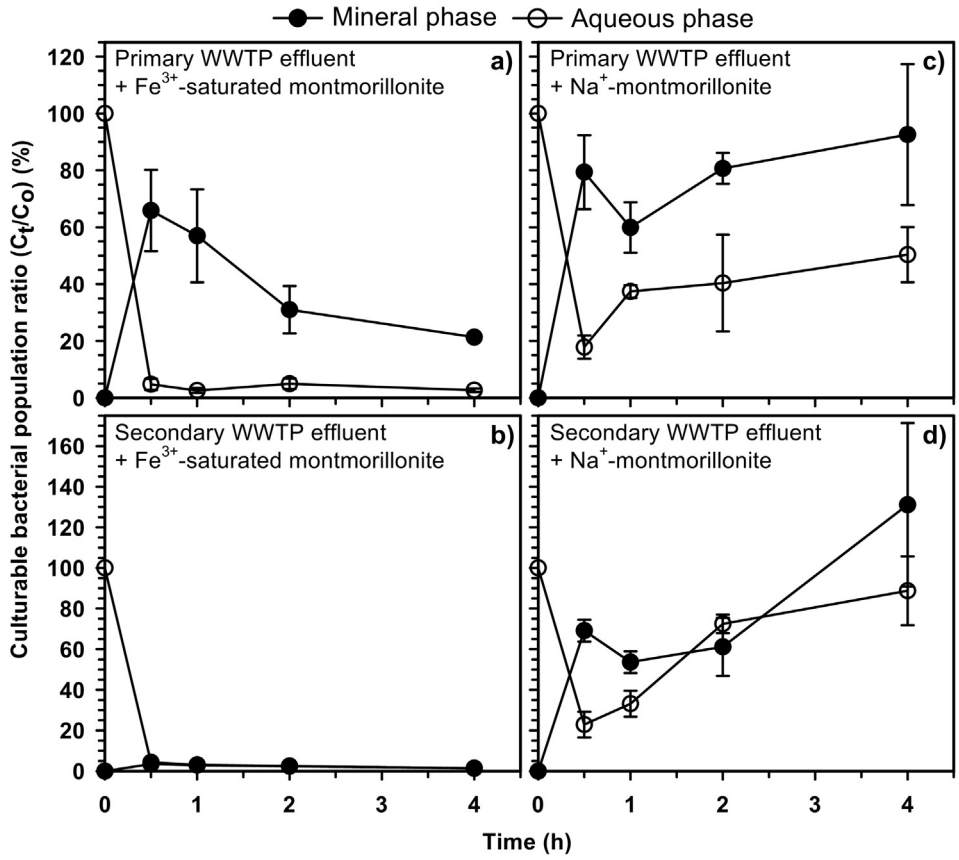

Fig. 3. Distribution of culturable bacterial population in aqueous phase and mineral phase after exposing the primary and secondary wastewater effluents to Fe^{3+}-saturated montmorillonite (left panels) and Na^{+}-montmorillonite (right panels) at 35 mg/mL for different exposure lengths. C_t is the culturable bacterial population at time t and C_o is the initial culturable bacterial population in a wastewater sample before exposure. The initial bacterial levels in the primary and secondary effluents were $(1.39 \pm 0.0862) \times 10^5$ and $(2.33 \pm 0.201) \times 10^4$ CFU/mL, respectively.

deactivation of surface sorbed bacteria is a slower process comparing to what were observed for the secondary wastewater effluent (Fig. 3b).

When the ratio of initial bacterial population to Fe^{3+}-saturated montmorillonite was low enough to achieve >90% deactivation efficiency (Fig. 2a), such as the case when secondary wastewater effluent was exposed to Fe^{3+}-saturated montmorillonite, bacteria sorbed on the mineral surfaces were quickly deactivated within 30 min of exposure (Fig. 3b). At 30 min, only 3.5 ± 1.4% of the initial wastewater bacterial population were mineral phase-associated and viable. The population of mineral surface-associated viable bacteria remained statistically unchanged with exposure time longer than 30 min. Similar to the result of primary wastewater effluent experiment, the fraction of initial wastewater bacterial population that was viable in the aqueous phase remained low, at 4.3 ± 0.50% and 1.3 ± 0.30%, when the secondary wastewater effluent was exposed for 30 min and 4 h, respectively, to Fe^{3+}-saturated montmorillonite.

Contrary to the treatment with Fe^{3+}-saturated montmorillonite, significant sorption of bacteria occurred on the Na^{+}-montmorillonite surfaces within 30 min of its exposure to the wastewater effluents (Fig. 3c, d). After 30 min exposure of Na^{+}-montmorillonite to the primary and secondary wastewater effluents, the mineral phase-associated viable bacteria were 79 ± 13% and 69 ± 5.4% of the initial bacterial populations, respectively, while those remained viable in the aqueous phase were 18 ± 4.1% and 23 ± 6.3% of the initial bacterial populations, respectively. This result indicates negligible overall bacterial deactivation within 30 min exposure to Na^{+}-montmorillonite. Longer exposure time seemed to encourage bacterial growth on the Na^{+}-montmorillonite mineral surfaces (Fig. 3c, d). From 30 min to 4 h exposure of the primary and secondary wastewater effluents to Na^{+}-montmorillonite, the net growth of mineral phase-associated bacteria increased ~17% and ~90%, respectively, while that of aqueous phase-associated bacteria increased ~ 33% and 288%, respectively.

Because bacterial cell surfaces have negatively charged sites, they can be sorbed to montmorillonite surfaces via bridging by cations or hydrated cations, both of which are electrostatically attracted to the permanent negative charges on the mineral surfaces (Huang, 2008; Theng et al., 1995). It was reported that bridging cations with higher valence could enhance bacterial cell sorption on mineral surfaces than those with lower valence (Ruddick and Williams, 1972). For example, the amount of actinomycete cells sorbed on Fe^{3+}-treated sand was observed to be close to 90 times higher than that sorbed on Na^{+}-treated sand (Ruddick and Williams, 1972). As shown in Fig. 3a and c, after 30 min exposure the viable populations associated with Fe^{3+}-saturated montmorillonite and Na^{+}-montmorillonite were similar in the systems with the primary wastewater effluent. This result suggests that although Fe^{3+}-saturated montmorillonite has much higher sorption capacity for bacterial cells than Na^{+}-montmorillonite, within 30 min exposure a large population of bacterial cells sorbed on the Fe^{3+}-saturated montmorillonite surfaces were deactivated and become not viable for plate culture. Fig. 3a demonstrates continuous bacterial deactivation/overall growth suppression of bacteria sorbed on the Fe^{3+}-saturated montmorillonite surfaces, while the opposite trend is shown for those sorbed on the Na^{+}-montmorillonite surfaces (Fig. 3c, d). In the case for secondary wastewater effluent, the bacterial deactivation efficiency on the Fe^{3+}-saturated montmorillonite surfaces could be greatly enhanced (Fig. 3b) because this system had higher ratio of available mineral surface area/bacterial population than that for the primary wastewater effluent system.

When 20 mg Fe^{3+}-saturated montmorillonite (0.997 mmol sorbed Fe^{3+}/g montmorillonite) was used to treat 2 mL of secondary

wastewater, 0.25% of the Fe^{3+} adsorbed to the montmorillonite was released back to the aqueous phase as free form, resulting in an aqueous concentration of 1.4 μg/mL for the desorbed Fe^{3+}. To further prove that the observed efficient bacterial deactivation by Fe^{3+}-saturated montmorillonite is a surface process catalyzed by the Fe^{3+} sorbed on the mineral surfaces, appropriate amount of $FeCl_3$ was added to the secondary wastewater effluent to provide Fe^{3+} at a content of 1.4 μg/mL. No significant bacterial deactivation ($-9.3 \pm 3.9\%$) was observed within 2 h incubation in the $FeCl_3$-added secondary wastewater. Previous studies have suggested that direct contact between microbial cells and surface of antimicrobial materials is necessary for microbial deactivation (Kang et al., 2007). It was shown that microbial cell deactivation was mainly localized on the Cu^{2+}-montmorillonite surface and was not due to the limited amount of Cu^{2+} desorbed from the mineral (1.2–2.3% of overall exchanged Cu^{2+}) into solution (Hu et al., 2005).

Adding Fe^{3+}-saturated montmorillonite (25 mg/mL) to wastewater lowered the pH from 7.2 to 3.3, which did not occur when adding Na^{+}-montmorillonite to the wastewater. However, our tests showed that this reduction of pH did not result in significant bacterial deactivation in the aqueous phase within the experimental time (Fig. S1). Both tests strongly support the argument that mineral surface activity of Fe^{3+}-saturated montmorillonite attributed to the observed overall bacterial deactivation in the system, while change of aqueous phase chemistry due to exposure to the mineral was not a contributing factor.

3.3. Spectroscopy evidence of bacterial cell deactivation on Fe^{3+}-saturated montmorillonite surfaces

The fluorescence image of Fig. 4a shows live and uniformly dispersed free bacterial cells in the wastewater before they were exposed to Fe^{3+}-saturated montmorillonite. When they were exposed to Na^{+}-montmorillonite and Fe^{3+}-saturated montmorillonite, the bacterial cells adhered onto the mineral surfaces as shown by the bacteria-mineral particle clusters in Fig. 4b and c, although the clusters for the former are less agglomerated. The green color bacteria-mineral clusters shown in Fig. 4b suggests that the bacterial cells sorbed on Na^{+}-montmorillonite were alive and viable. The bacterial cells sorbed on Fe^{3+}-saturated montmorillonite were clearly shown to be non-viable as indicated by the red color in the fluorescence image (Fig. 4c). The results from Fig. 4 strongly suggested that once bacterial cells were sorbed onto Fe^{3+}-saturated montmorillonite surfaces, bacterial membranes were most likely disrupted by a chemical mechanism involving the surface saturated Fe^{3+}, resulting in nonviable cells as shown in red. Further scanning electron microscopy (SEM) investigation would provide direct spectroscopic evidence on cell integrity (Hoque et al., 2015; Ma et al., 2015; Tang et al., 2013).

In general, bacterial deactivation can be the result of: 1) direct mechanical breakage of outer cell membranes by sharp edged nanoparticles (Akhavan and Ghaderi, 2010; Liu et al., 2009; Situ and Samia, 2014); 2) chemical oxidative stress mediated cell injury that is induced by in situ production of reactive oxygen species (Krishnamoorthy et al., 2012; Su et al., 2009); and 3) dehydration of cell membrane (Beney et al., 2004). It is highly likely that the latter two bacterial deactivation mechanisms are at play when wastewater is exposed to Fe^{3+}-saturated montmorillonite. Recent research has shown mineral surface-catalyzed Fe^{3+} reduction by organic phenolic compounds exposed to Fe^{3+}-saturated montmorillonite, forming radical cations of aromatic molecules and Fe^{2+} cations (Gu et al., 2008; Liyanapatirana et al., 2009; Polubesova et al., 2010; Qin et al., 2014). Hence, the surface-catalyzed redox reaction and formation of radical cations could possibly induce oxidative stress on bacterial cells, resulting in disrupted bacterial cell membrane and subsequent bacterial deactivation. In addition, strong hydration force of surface sorbed Fe^{3+} could quickly induce cell membrane dehydration of bacterial cells sorbed on the montmorillonite surfaces. However, to pinpoint the exact bacterial deactivation mechanism(s) of Fe^{3+}-saturated montmorillonite, more studies are needed to investigate the changes of cell morphology using spectroscopic methods, to monitor reactive oxygen species production, and to understand metabolic and physiological activity of bacterial cells in aqueous systems with the presence of Fe^{3+}-saturated montmorillonite.

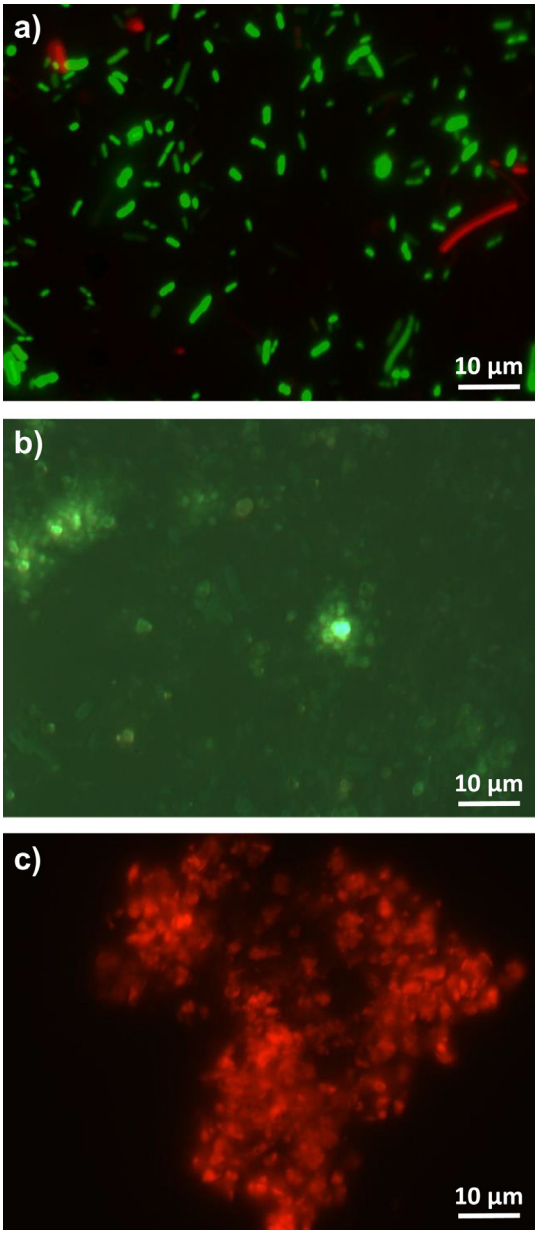

Fig. 4. Representative fluorescence microscope images of bacteria in a wastewater sample before exposure (a) and after exposure to Na^{+}-montmorillonite (b) and Fe^{3+}-saturated montmorillonite (c) at 25 mg/mL for 4 h. The initial average level of cultured bacterial in the wastewater effluents was 3.6×10^9 CFU/mL.

3.4. Reusability of Fe^{3+}-saturated montmorillonite for bacterial deactivation in wastewater

To test the reusability of Fe^{3+}-saturated montmorillonite, an experiment consisting of four consecutive 2-h long exposures of the same batches of Fe^{3+}-saturated montmorillonite at an exposure rate of 25 mg/mL to fresh secondary wastewater effluent was conducted. After each exposure, the aqueous phase and mineral phase were separated and the mineral phase was used as is or freeze dried before the next round of exposure to a new batch of wastewater. Bacterial

deactivation efficiencies were 97 ± 0.58%, 86 ± 2.3%, 69 ± 2.6%, and 57 ± 12% for the 1st, 2nd, 3rd, and 4th exposure, respectively, where the Fe^{3+}-saturated montmorillonite was collected and used as is after each exposure (Fig. 5). This decline of bacterial deactivation efficiency with subsequent repeated use of the same used-as-is Fe^{3+}-saturated montmorillonite might be due to the blockage of the mineral surface reaction sites by the deactivated bacterial cells remaining on the mineral surface from the previous exposure. However, when the Fe^{3+}-saturated montmorillonite was freeze-dried before each reuse, its bacterial deactivation efficiency remained at 82 ± 0.51% even when it was reused four consecutive times (Fig. 5). Dehydration of the reused Fe^{3+}-saturated montmorillonite during freeze-drying process might help weaken the attraction between deactivated bacterial cells and the mineral surfaces, resulting in their detachment from the mineral surfaces once re-exposed to the aqueous phase and, therefore, freeing up the reactive sites for further bacterial deactivation. The freeze-drying followed by quick hydration might also enhance the physical removal of other coated species from wastewater.

4. Conclusion

In summary, this study demonstrated the effectiveness of Fe^{3+}-saturated montmorillonite for bacterial deactivation in secondary wastewater effluent. Bacterial deactivation efficiency was 92 ± 0.64% when a secondary wastewater effluent was mixed with Fe^{3+}-saturated montmorillonite at 35 mg/mL for 30 min, and further reached to 97 ± 0.61% after 4-h exposure. This deactivation efficiency was similar to that obtained when the same wastewater was subjected to UV-disinfection. It was estimated that the ratio between wastewater bacterial population and mass of Fe^{3+}-saturated montmorillonite at $<2 \times 10^3$ CFU/mg would achieve >90% bacterial deactivation efficiency, which is comparable to that of UV disinfection. Bacterial cultural results coupled with the live/dead fluorescent staining assay observation strongly suggests that Fe^{3+}-saturated montmorillonite deactivated bacteria in wastewater through the following two possible steps: electrostatic sorption of bacterial cells to the surfaces of Fe^{3+}-saturated montmorillonite, followed by bacterial deactivation due to surface-catalyzed bacterial cell membrane disruption by the surface saturated Fe^{3+}. This study strongly suggests that Fe^{3+}-saturated montmorillonite could be possibly used as effective anti-bacterial material for water disinfection in applications from small scale point-of-use drinking water treatment devices to large scale drinking and wastewater treatment facilities.

Supplementary data to this article can be found online at https://doi.org/10.1016/j.scitotenv.2017.11.302.

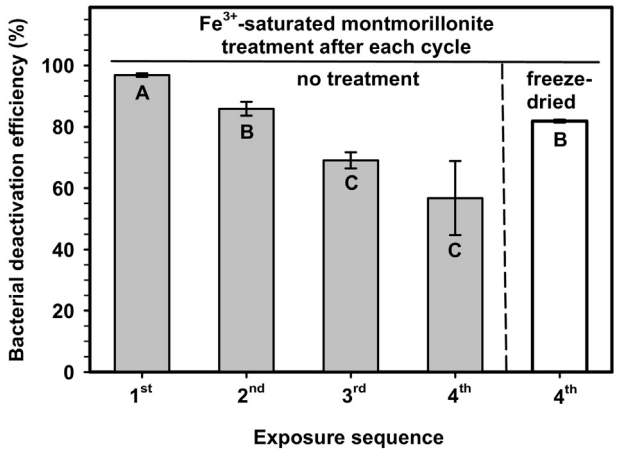

Fig. 5. Bacterial deactivation efficiency of Fe^{3+}-saturated montmorillonite used repetitively for four consecutive 2-h exposures. A fresh batch of secondary wastewater effluent was used for each exposure. The Fe^{3+}-saturated montmorillonite exposure dose was 25 mg/mL. The initial bacterial level in secondary effluent was $(7.90 \pm 1.14) \times 10^4$ CFU/mL. The Fe^{3+} saturated montmorillonite was collected via centrifugation and used as is (left panel) or freeze-dried (right panel) after each exposure. Capital letter within each bar indicates statistical difference at a significance level of $p < 0.05$ within a 95% confidence interval.

Acknowledgements

We acknowledge the financial support from USDA NIFA award #2013-67019-21355. Funding for this work was provided, in part, by the Virginia Agricultural Experiment Station and the Hatch Program of the National Institute of Food and Agriculture, U.S. Department of Agriculture. We thank Mr. Bobby Epperly from Blacksburg-VPI Sanitation Authority Treatment Plant for assistance with wastewater sample collection. We also thank Dr. Kristi DeCourcy from the Imaging Center at Virginia Tech Fralin Life Science Institute for assistance with the fluorescence microscope.

References

Akhavan, O., Ghaderi, E., 2010. Toxicity of graphene and graphene oxide nanowalls against bacteria. ACS Nano 4, 5731–5736.
APHA, 2012. Standard Methods for the Examination of Water and Wastewater. APHA, AWWA, WPC, Washington, DC.
Applerot, G., Lipovsky, A., Dror, R., Perkas, N., Nitzan, Y., Lubart, R., et al., 2009. Enhanced antibacterial activity of nanocrystalline ZnO due to increased ROS-mediated cell injury. Adv. Funct. Mater. 19, 842–852.
Beney, L., Mille, Y., Gervais, P., 2004. Death ofEscherichia coli during rapid and severe dehydration is related to lipid phase transition. Appl. Microbiol. Biotechnol. 65, 457–464.
Ben-Sasson, M., Zodrow, K.R., Genggeng, Q., Kang, Y., Giannelis, E.P., Elimelech, M., 2013. Surface functionalization of thin-film composite membranes with copper nanoparticles for antimicrobial surface properties. Environ. Sci. Technol. 48, 384–393.
Dankovich, T.A., Gray, D.G., 2011. Bactericidal paper impregnated with silver nanoparticles for point-of-use water treatment. Environ. Sci. Technol. 45, 1992–1998.
Feng, Q.L., Wu, J., Chen, G.Q., Cui, F.Z., Kim, T.N., Kim, J.O., 2000. A mechanistic study of the antibacterial effect of silver ions on *Escherichia coli* and *Staphylococcus aureus*. J. Biomed. Mater. Res. 52, 662–668.
Gu, C., Li, H., Teppen, B.J., Boyd, S.A., 2008. Octachlorodibenzodioxin formation on Fe (III)-montmorillonite clay. Environ. Sci. Technol. 42, 4758–4763.
Hoque, J., Akkapeddi, P., Yadav, V., Manjunath, G.B., Uppu, D.S.S.M., Konai, M.M., et al., 2015. Broad Spectrum antibacterial and antifungal polymeric paint materials: synthesis, structure–activity relationship, and membrane-active mode of action. ACS Appl. Mater. Interfaces 7, 1804–1815.
Hrenovic, J., Milenkovic, J., Ivankovic, T., Rajic, N., 2012. Antibacterial activity of heavy metal-loaded natural zeolite. J. Hazard. Mater. 201, 260–264.
Hu, C.H., ZR, Xu, Xia, M.S., 2005. Antibacterial effect of Cu^{2+}-exchanged montmorillonite on *Aeromonas hydrophila* and discussion on its mechanism. Vet. Microbiol. 109, 83–88.
Hu, W., Peng, C., Luo, W., Lv, M., Li, X., Li, D., et al., 2010. Graphene-based antibacterial paper. ACS Nano 4, 4317–4323.
Huang, P., 2004. Soil mineral–organic matter–microorganism interactions: fundamentals and impacts. Adv. Agron. 82, 391–472.
Huang, P.M., 2008. Impacts of physicochemical-biological interactions on metal and metalloid transformations in soils: an overview (P.M. Huang). In: Violante, A., Huang, P.M., Gadd, G.M. (Eds.), Biophysico-Chemical Processes of Heavy Metals and Metalloids in Soil Environments. Wiley Interscience, pp. 3–52.
Huang, W.J., Fang, G.C., Wang, C.C., 2005. The determination and fate of disinfection by-products from ozonation of polluted raw water. Sci. Total Environ. 345, 261–272.
Kang, S., Pinault, M., Pfefferle, L.D., Elimelech, M., 2007. Single-walled carbon nanotubes exhibit strong antimicrobial activity. Langmuir 23, 8670–8673.
Katsoyiannis, A., Samara, C., 2007. The fate of dissolved organic carbon (DOC) in the wastewater treatment process and its importance in the removal of wastewater contaminants. Environ. Sci. Pollut. Res. Int. 14, 284–292.
Krasner, S.W., Westerhoff, P., Chen, B., Rittmann, B.E., Amy, G., 2009. Occurrence of disinfection byproducts in United States wastewater treatment plant effluents. Environ. Sci. Technol. 43, 8320–8325.
Krishnamoorthy, K., Veerapandian, M., Zhang, L.-H., Yun, K., Kim, S.J., 2012. Antibacterial efficiency of graphene nanosheets against pathogenic bacteria via lipid peroxidation. J. Phys. Chem. C 116, 17280–17287.
Li, Y., Zhang, W., Niu, J., Chen, Y., 2012. Mechanism of photogenerated reactive oxygen species and correlation with the antibacterial properties of engineered metal-oxide nanoparticles. ACS Nano 6, 5164–5173.
Liu, S., Wei, L., Hao, L., Fang, N., Chang, M.W., Xu, R., et al., 2009. Sharper and faster "nano darts" kill more bacteria: a study of antibacterial activity of individually dispersed pristine single-walled carbon nanotube. ACS Nano 3, 3891–3902.
Liu, S., Zeng, T.H., Hofmann, M., Burcombe, E., Wei, J., Jiang, R., et al., 2011. Antibacterial activity of graphite, graphite oxide, graphene oxide, and reduced graphene oxide: membrane and oxidative stress. ACS Nano 5, 6971–6980.
Liu, S., Hu, M., Zeng, T.H., Wu, R., Jiang, R., Wei, J., et al., 2012. Lateral dimension-dependent antibacterial activity of graphene oxide sheets. Langmuir 28, 12364–12372.

Liyanapatirana, C., Gwaltney, S.R., Xia, K., 2009. Transformation of triclosan by Fe (III)-saturated montmorillonite. Environ. Sci. Technol. 44, 668–674.
Lv, M., Su, S., He, Y., Huang, Q., Hu, W., Li, D., et al., 2010. Long-term antimicrobial effect of silicon nanowires decorated with silver nanoparticles. Adv. Mater. 22, 5463–5467.
Lyon, D.Y., Alvarez, P.J.J., 2008. Fullerene water suspension (nC60) exerts antibacterial effects via ROS-independent protein oxidation. Environ. Sci. Technol. 42, 8127–8132.
Ma, S., Zhan, S., Jia, Y., Zhou, Q., 2015. Superior antibacterial activity of Fe3O4-TiO2 nanosheets under solar light. ACS Appl. Mater. Interfaces 7, 21875–21883.
Magana, S.M., Quintana, P., Aguilar, D.H., Toledo, J.A., Angeles-Chavez, C., Cortes, M.A., et al., 2008. Antibacterial activity of montmorillonites modified with silver. J. Mol. Catal. A Chem. 281, 192–199.
Malachová, K., Praus, P., Rybková, Z., Kozák, O., 2011. Antibacterial and antifungal activities of silver, copper and zinc montmorillonites. Appl. Clay Sci. 53, 642–645.
Matsumura, Y., Yoshikata, K., Kunisaki, S.-i., Tsuchido, T., 2003. Mode of bactericidal action of silver zeolite and its comparison with that of silver nitrate. Appl. Environ. Microbiol. 69, 4278–4281.
Meghana, S., Kabra, P., Chakraborty, S., Padmavathy, N., 2015. Understanding the pathway of antibacterial activity of copper oxide nanoparticles. RSC Adv. 5, 12293–12299.
Morones, J.R., Elechiguerra, J.L., Camacho, A., Holt, K., Kouri, J.B., Ramírez, J.T., et al., 2005. The bactericidal effect of silver nanoparticles. Nanotechnology 16, 2346.
Morrison, K.D., Underwood, J.C., Metge, D.W., Eberl, D.D., Williams, L.B., 2014. Mineralogical variables that control the antibacterial effectiveness of a natural clay deposit. Environ. Geochem. Health 36, 613–631.
Muller, A., Weiss, S.C., Beisswenger, J., Leukhardt, H.G., Schulz, W., Seitz, W., et al., 2012. Identification of ozonation by-products of 4- and 5-methyl-1H-benzotriazole during the treatment of surface water to drinking water. Water Res. 46, 679–690.
Panáček, A., Kvitek, L., Prucek, R., Kolar, M., Vecerova, R., Pizurova, N., et al., 2006. Silver colloid nanoparticles: synthesis, characterization, and their antibacterial activity. J. Phys. Chem. B 110, 16248–16253.
Pepper, I.L., Gerba, C.P., 2015. Chapter 10 - cultural methods. Environmental Microbiology, Third edition Academic Press, San Diego, pp. 195–212.
Perreault, F., de Faria, A.F., Nejati, S., Elimelech, M., 2015. Antimicrobial properties of graphene oxide nanosheets: why size matters. ACS Nano 9, 7226–7236.
Polubesova, T., Eldad, S., Chefetz, B., 2010. Adsorption and oxidative transformation of phenolic acids by Fe (III)-montmorillonite. Environ. Sci. Technol. 44, 4203–4209.
Qin, C., Troya, D., Shang, C., Hildreth, S., Helm, R., Xia, K., 2014. Surface catalyzed oxidative oligomerization of 17β-estradiol by Fe^{3+}-saturated montmorillonite. Environ. Sci. Technol. 49, 956–964.
Qu, X., Brame, J., Li, Q., Alvarez, P.J.J., 2012. Nanotechnology for a safe and sustainable water supply: enabling integrated water treatment and reuse. Acc. Chem. Res. 46, 834–843.
Raghupathi, K.R., Koodali, R.T., Manna, A.C., 2011. Size-dependent bacterial growth inhibition and mechanism of antibacterial activity of zinc oxide nanoparticles. Langmuir 27, 4020–4028.
Richardson, S.D., Postigo, C., 2011. Drinking water disinfection by-products. Emerging organic contaminants and human health. Spring 93–137.
Ruddick, S.M., Williams, S.T., 1972. Studies on the ecology of actinomycetes in soil V. Some factors influencing the dispersal and adsorption of spores in soil. Soil Biol. Biochem. 4, 93 (IN7, 101–100, IN10, 103).
Shannon, M.A., Bohn, P.W., Elimelech, M., Georgiadis, J.G., Mariñas, B.J., Mayes, A.M., 2008. Science and technology for water purification in the coming decades. Nature 452, 301–310.
Simon-Deckers, A., Loo, S., Mayne-L'hermite, M., Herlin-Boime, N., Menguy, N., Reynaud, C., et al., 2009. Size-, composition-and shape-dependent toxicological impact of metal oxide nanoparticles and carbon nanotubes toward bacteria. Environ. Sci. Technol. 43, 8423–8429.
Situ, S.F., Samia, A.C.S., 2014. Highly efficient antibacterial iron oxide@ carbon nanochains from wustite precursor nanoparticles. ACS Appl. Mater. Interfaces 6, 20154–20163.
Stotzky, G., 1966. Influence of clay minerals on microorganisms: ii. Effect of various clay species, homoionic clays, and other particles on bacteria. Can. J. Microbiol. 12, 831–848.
Stotzky, G., Rem, L.T., 1966. Influence of clay minerals on microorganisms: I. Montmorillonite and kaolinite on bacteria. Can. J. Microbiol. 12, 547–563.
Su, H.-L., Chou, C.-C., Hung, D.-J., Lin, S.-H., Pao, I.-C., Lin, J.-H., et al., 2009. The disruption of bacterial membrane integrity through ROS generation induced by nanohybrids of silver and clay. Biomaterials 30, 5979–5987.
Tang, J., Chen, Q., Xu, L., Zhang, S., Feng, L., Cheng, L., et al., 2013. Graphene oxide–silver nanocomposite as a highly effective antibacterial agent with species-specific mechanisms. ACS Appl. Mater. Interfaces 5, 3867–3874.
Theng, K., Orchard, V., Huang, P., Berthelin, J., Bollag, J., McGill, W., et al., 1995. Interactions of Clays With Microorganisms and Bacterial Survival in Soil: A Physicochemical Perspective. Environmental Impact of Soil Component Interactions: Volume 2: Metals, Other Inorganics, and Microbial Activities. pp. 123–143.
Tiraferri, A., Vecitis, C.D., Elimelech, M., 2011. Covalent binding of single-walled carbon nanotubes to polyamide membranes for antimicrobial surface properties. ACS Appl. Mater. Interfaces 3, 2869–2877.
Tong, G., Yulong, M., Peng, G., Zirong, X., 2005. Antibacterial effects of the Cu (II)-exchanged montmorillonite on *Escherichia coli* K88 and *Salmonella choleraesuis*. Vet. Microbiol. 105, 113–122.
Van Loosdrecht, M.C., Lyklema, J., Norde, W., Zehnder, A.J., 1990. Influence of interfaces on microbial activity. Microbiol. Rev. 54, 75–87.
Vecitis, C.D., Zodrow, K.R., Kang, S., Elimelech, M., 2010. Electronic-structure-dependent bacterial cytotoxicity of single-walled carbon nanotubes. ACS Nano 4, 5471–5479.
Williams, L.B., Haydel, S.E., 2010. Evaluation of the medicinal use of clay minerals as antibacterial agents. Int. Geol. Rev. 52, 745–770.
Wu, M.-C., Deokar, A.R., Liao, J.-H., Shih, P.-Y., Ling, Y.-C., 2013. Graphene-based photothermal agent for rapid and effective killing of bacteria. ACS Nano 7, 1281–1290.
Zha, X.S., Liu, Y., Liu, X., Zhang, Q., Dai, R.H., Ying, L.W., et al., 2014. Effects of bromide and iodide ions on the formation of disinfection by-products during ozonation and subsequent chlorination of water containing biological source matters. Environ. Sci. Pollut. Res. Int. 21, 2714–2723.
Zhou, Y., Jiang, X., Tang, J., Su, Y., Peng, F., Lu, Y., et al., 2014. A silicon-based antibacterial material featuring robust and high antibacterial activity. J. Mater. Chem. B 2, 691–697.